Improvement of Forest Canopy Characterization Based on NoahMP and Its Impact on Land Air Exchange Processes

Ming Chang
changming@email.jnu.edu.cn
Jinan University, Guangzhou, China
Collaborators: Guotong Wu, Wenxin Lin, Xinyuan Kang, Xuemei Wang

Noah-MP workshop, 4 Jun 2024

Key processes: land-air exchange

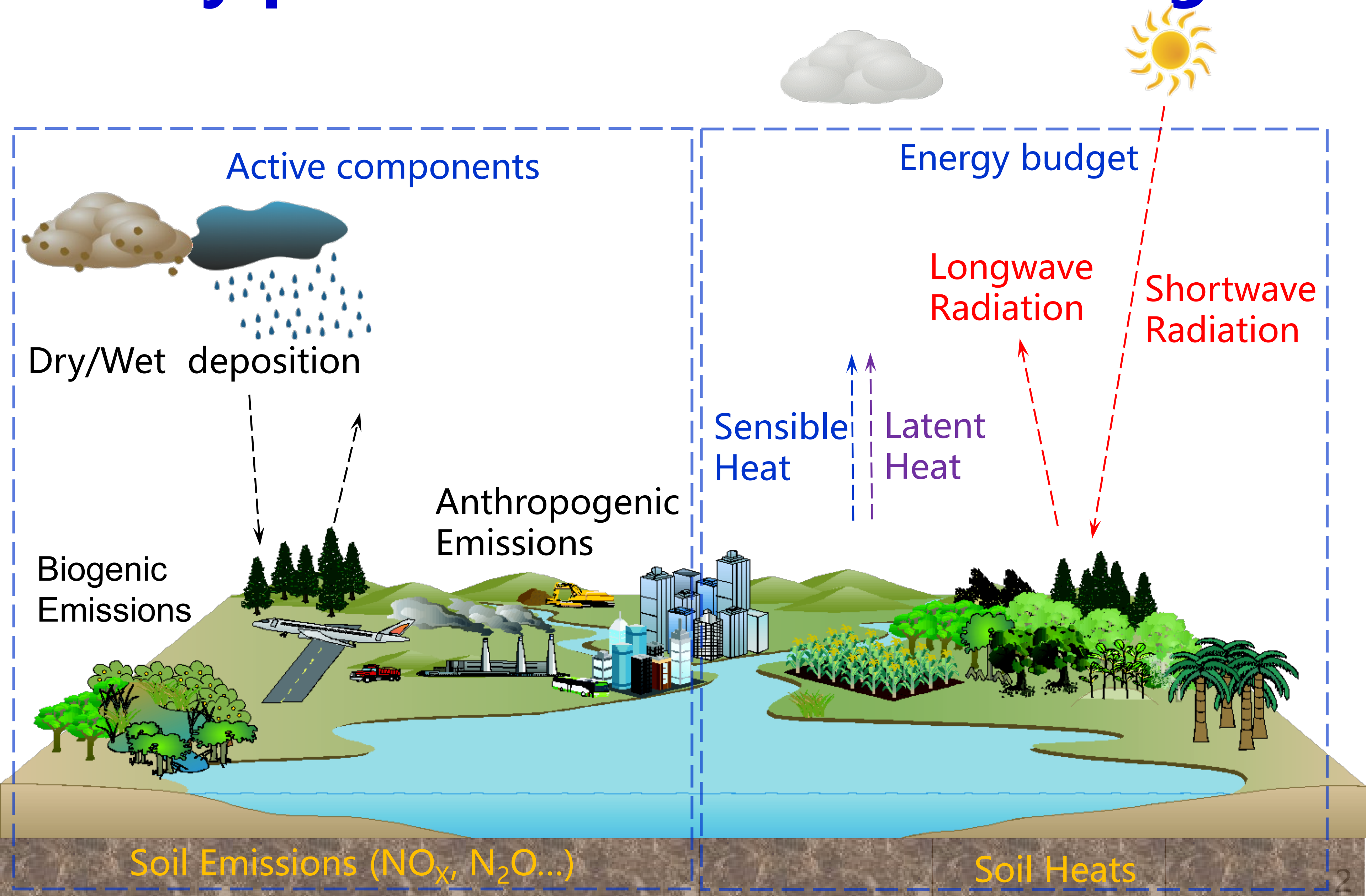

Key interface: canopy

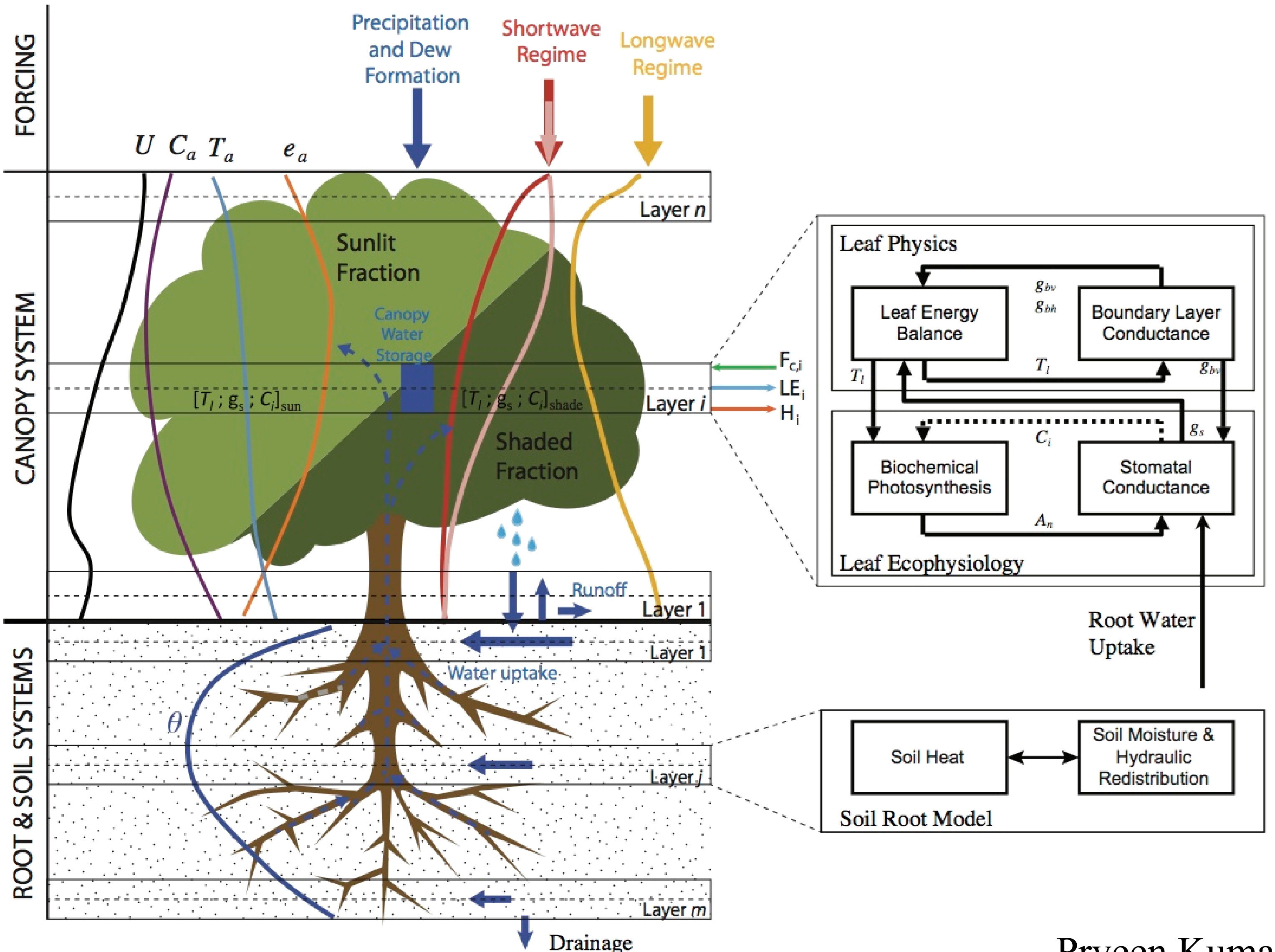

Prveen Kumar, 2013

Vegetation morphology in different models

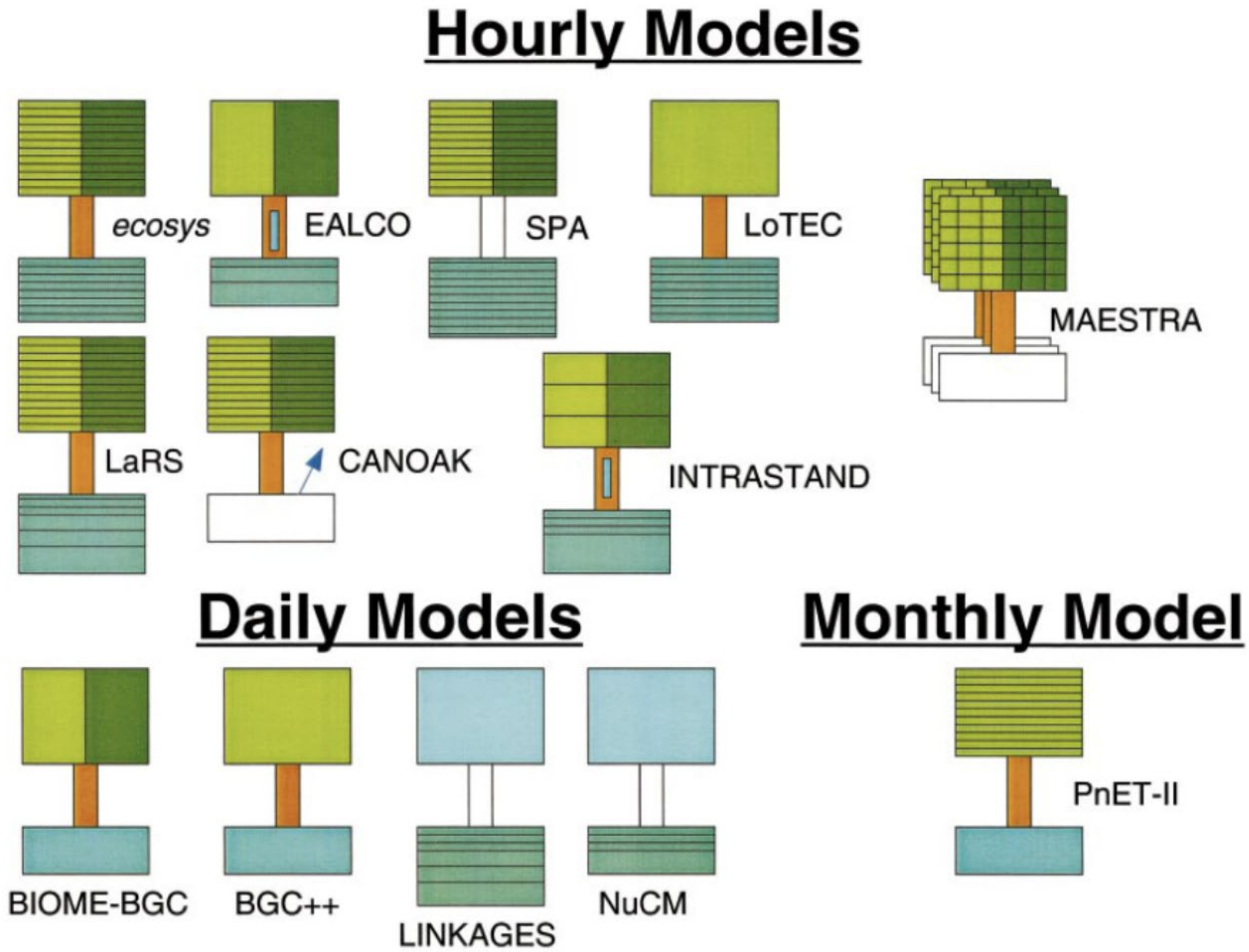

Hanson et al, 2004; D. Baldocchi., 2016

Parameters of Canopy in Noah-MP

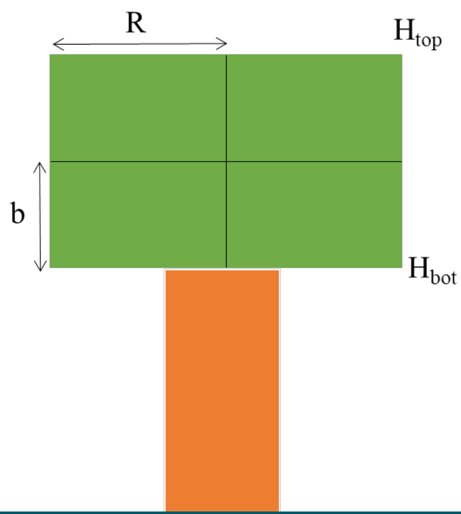

- Phenology
- Radiation distribution
- Stomata processes
- Turbulent ……

The canopy structure is represented by a simple geometric shape

MPTABLE.TBL

NAME	Used/Defined in Subroutine	Short description [units]
CH2OP	CANWATER	Maximum water intercepted by canopy [mm]
DLEAF	RAGRB	Leaf dimension [m]
Z0MVT	ENERGY	Momentum roughness length [m]
HVT	PHENOLOGY / TWOSTREAM	Canopy top [m]
HVB	PHENOLOGY / TWOSTREAM	Canopy bottom [m]
DEN	TWOSTREAM	Tree density [number/m^2]
RC	TWOSTREAM	Crown radius [m]
		… … … …
FOLNMX	CO2FLUX / STOMATA	Maximum foliage nitrogen factor (see FOLN setting in code) [unitless]
WDPOOL	CO2FLUX	Wood pool factor used to determine relative wood presence [unitless]
WRRAT	CO2FLUX	Wood to non-wood ratio [kg/kg]
MRP	CO2FLUX	Microbial respiration in fast soil carbon pool at 10^oC [umol/m^2/s]
SAIM	PHENOLOGY	Monthly stem area index when prescribed [m^2/m^2]
LAIM	PHENOLOGY	Monthly leaf area index when prescribed [m^2/m^2]
SLAREA	BVOCFLUX	Stem-to-leaf area density [unitless]
EPS	BVOCFLUX	Emission capacity for up to 5 different BVOC fluxes at 30^oC [ug C/g foliar mass/hour]

The canopy data by earth observation

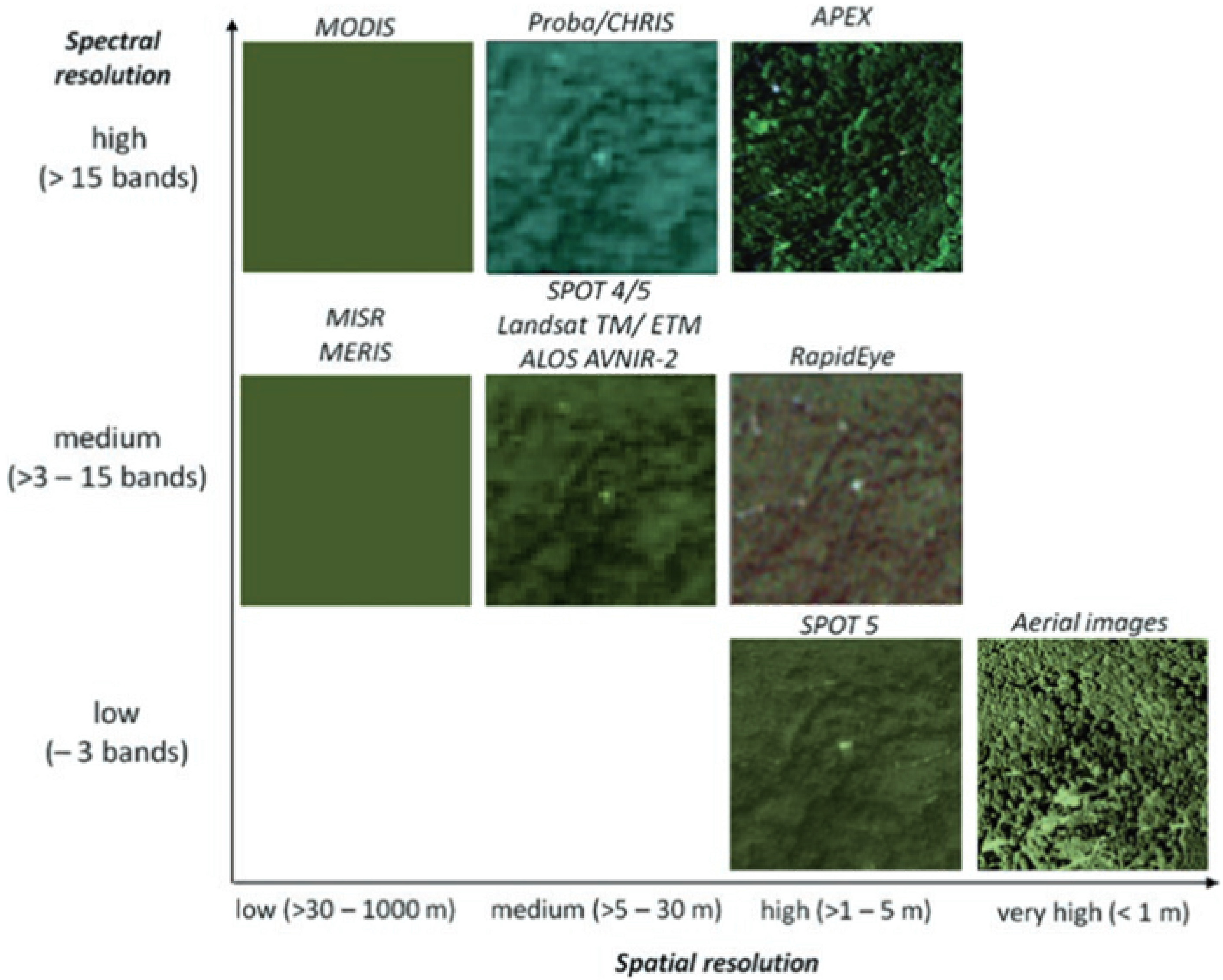

Felix M. et al., 2020

How to get canopy parameters in our study forest?

Sample site, Subtropical forests in Guangdong, China

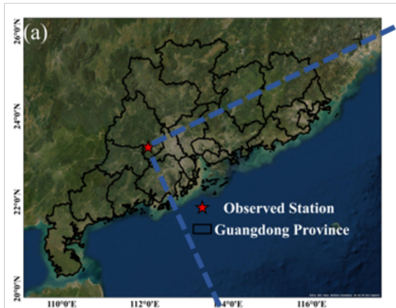

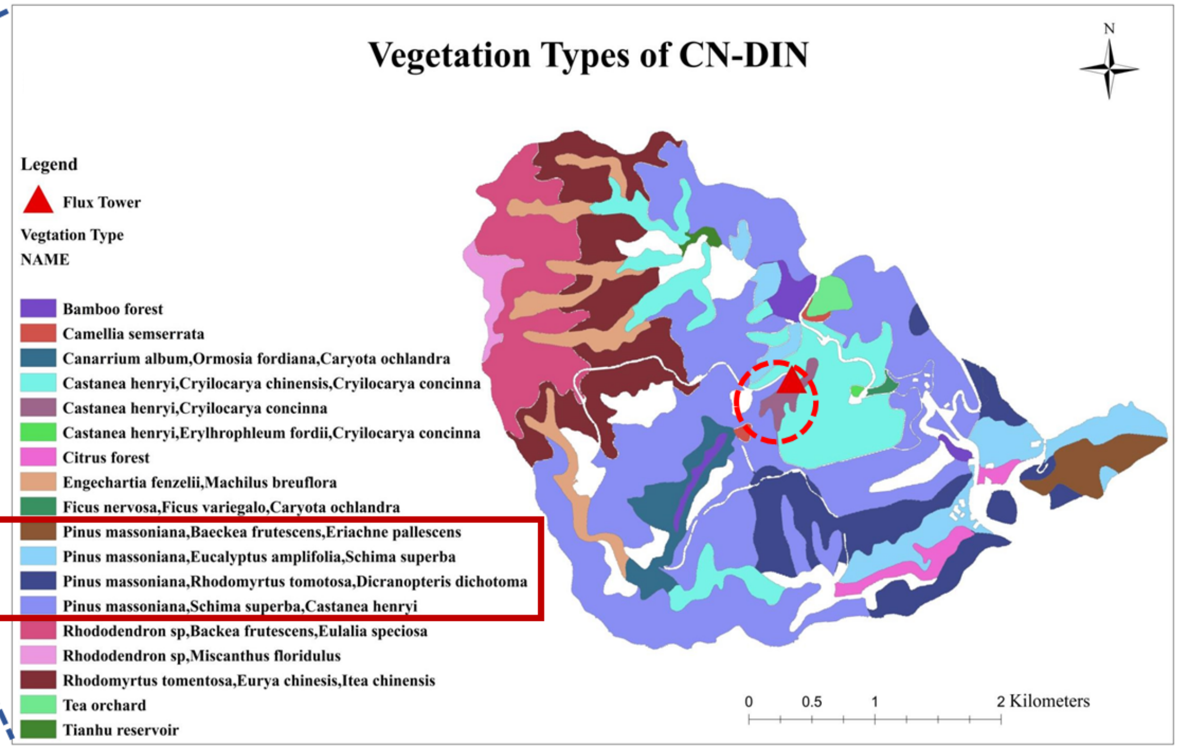

FluxTower

- The main tree species are Pinus massoniana.

Using UAV-based Photogrammetry

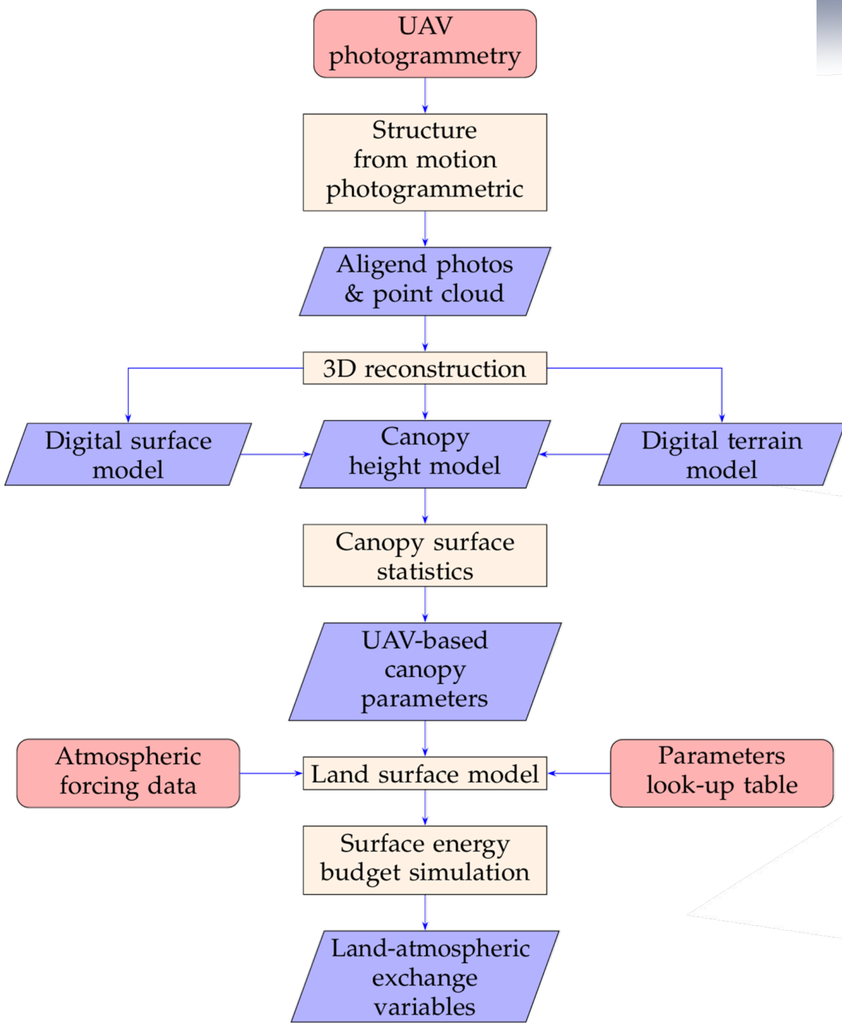

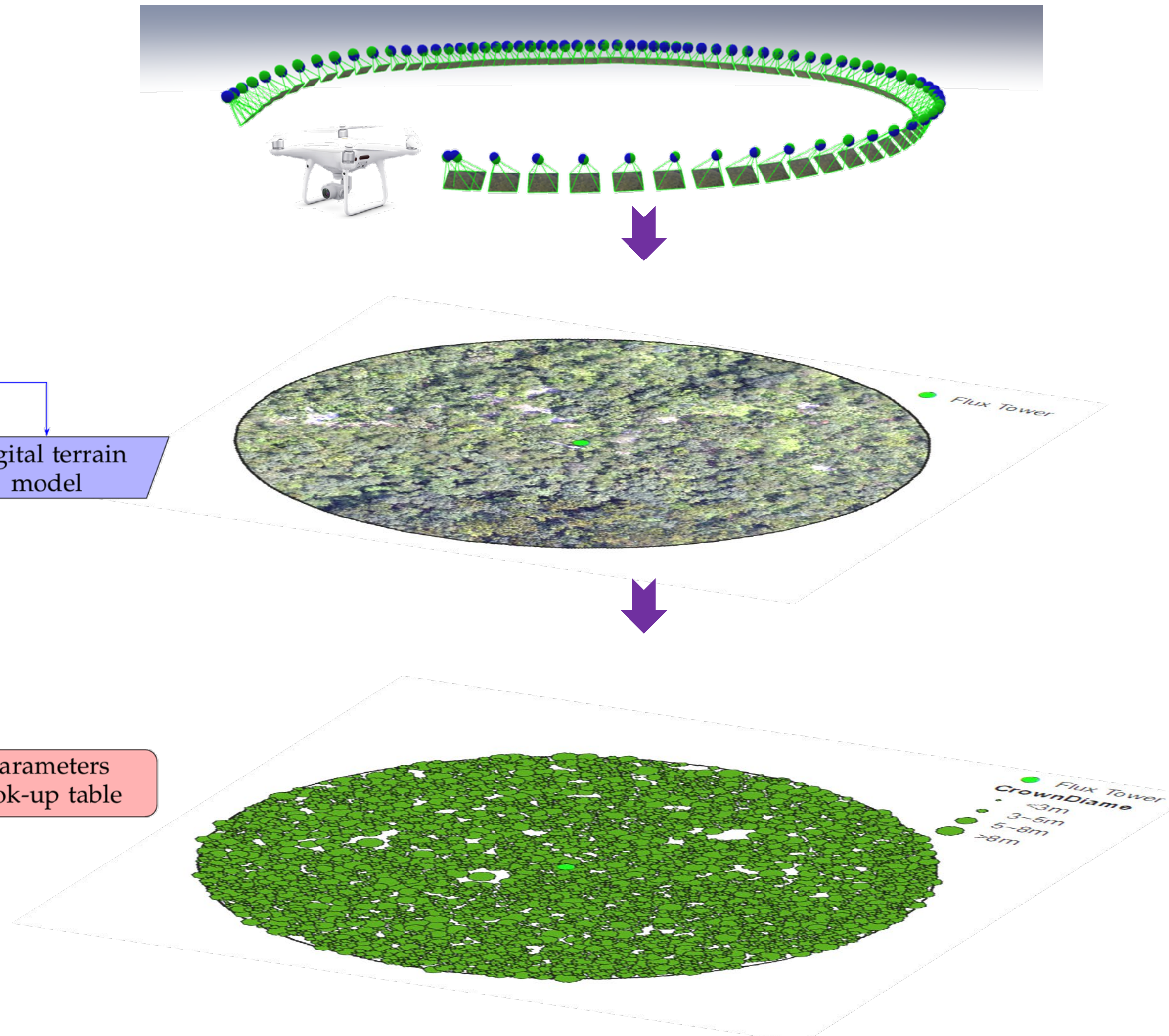

M Chang, et al. *Remote Sensing*. 2020

Correction of canopy parameters and its effects

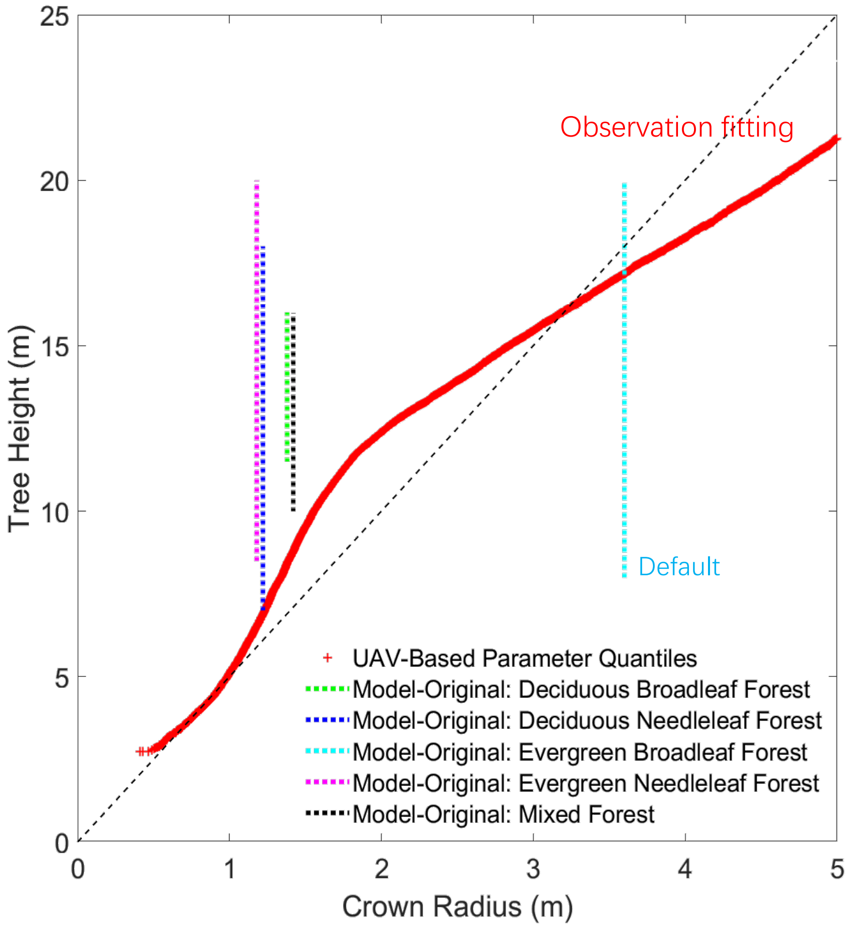

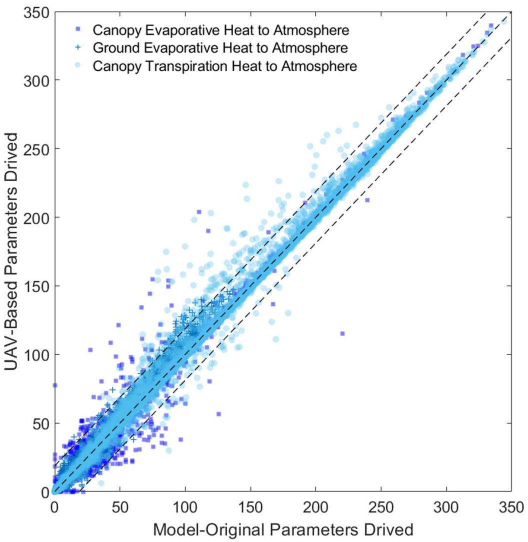

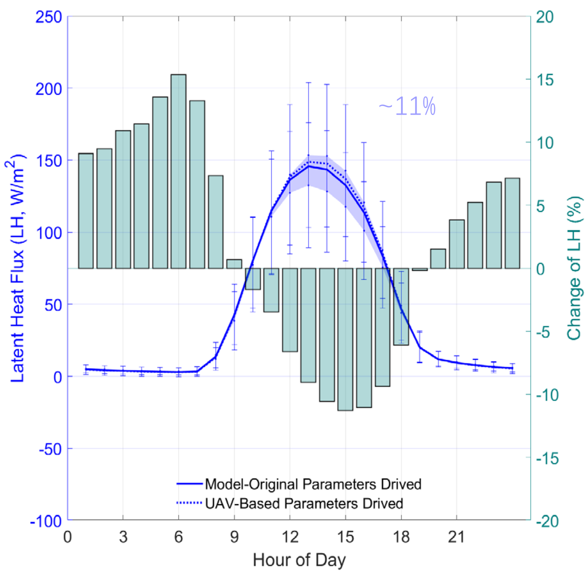

M Chang, et al. *Remote Sensing*. 2020

How to get more accuracy canopy parameters?

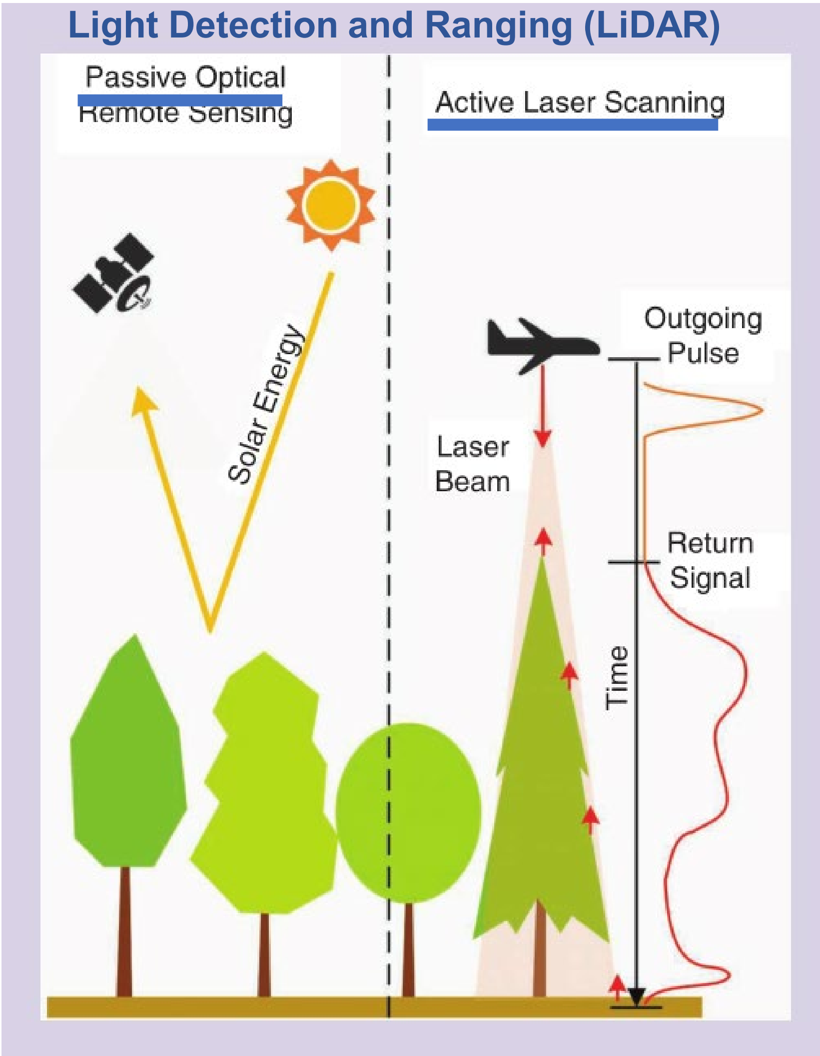

- **UAV and Airborne LiDAR:**
  - **High accuracy**
  - **High flexibility**
  - **Large range of acquired data**

- **Multiple echoes based on different altitudes for canopy.**
- **Less affected by occlusions and shadows, can penetrate the canopy and acquire three-dimensional information.**

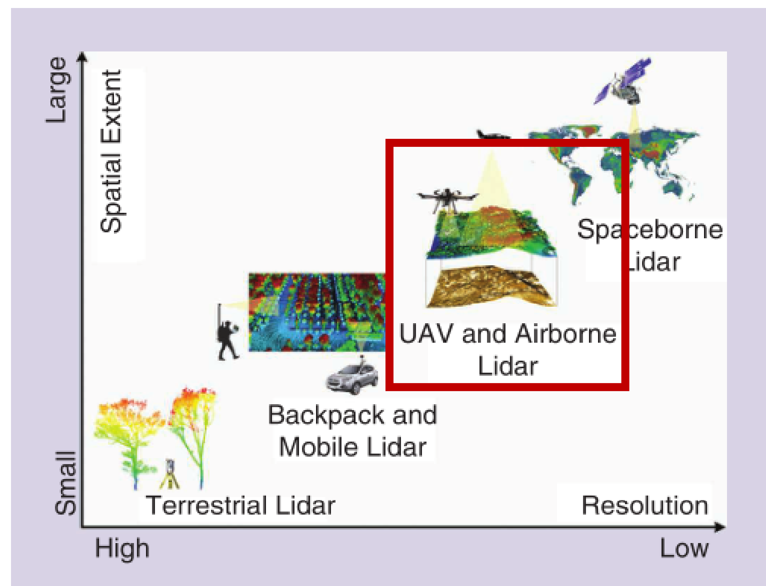

Guo et al., 2021

UAVs and LiDAR setup

- Active remote sensing: unmanned airborne lidar
- Passive optical remote sensing: visible light drones

- Heading overlap: 80.0%
- Scanning angle: 37° and 70°

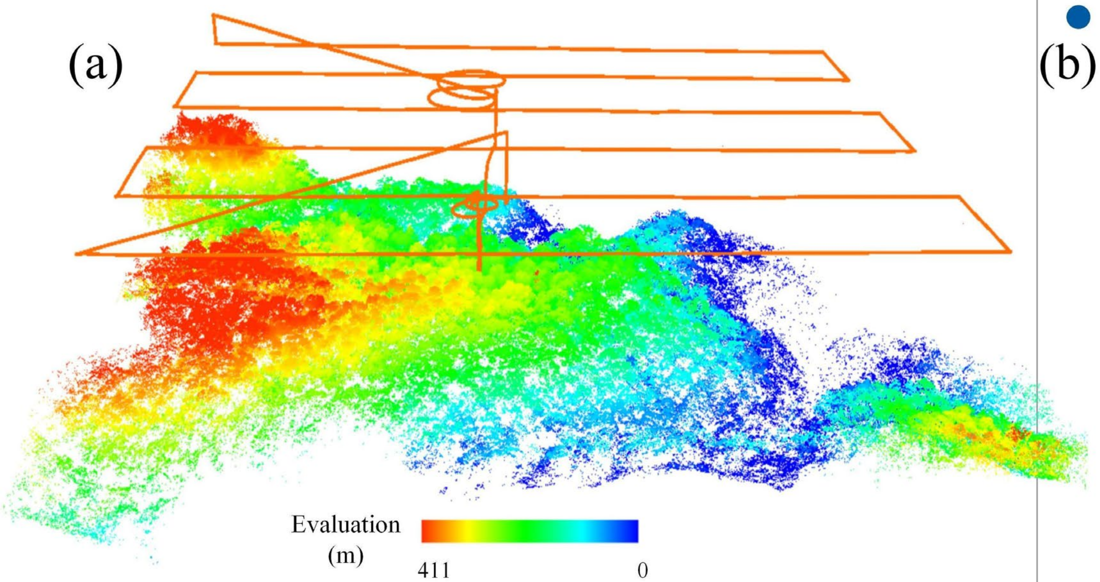

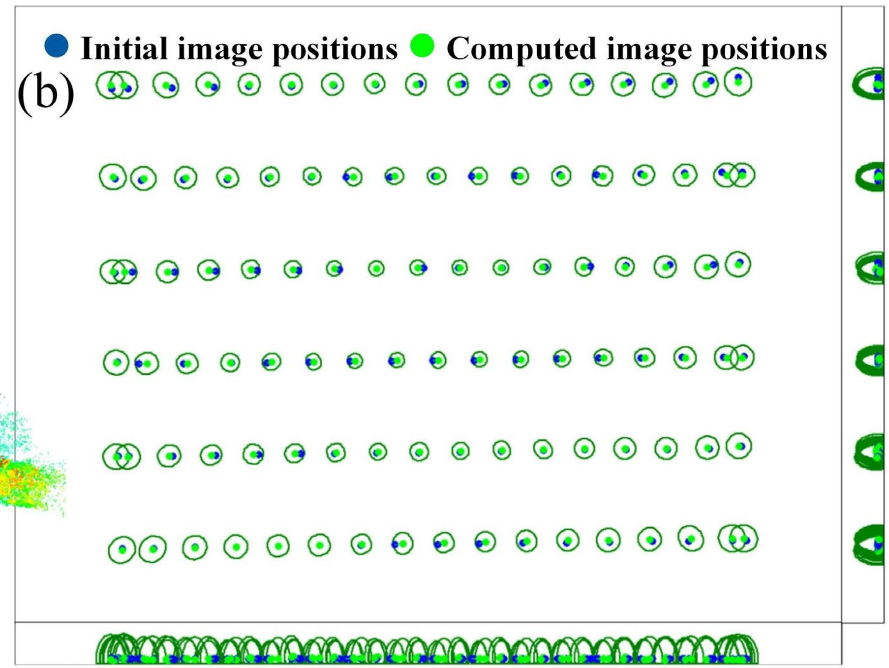

- Flight altitude: 100 metres from the landing site
- Flight speed: 4.3 m/s
- Average sampling distance: 7.24 cm

- Relative geographic accuracy

  X: 95.0% Y: 100.0% Z: 100.0%

Single Tree Segmentation of Point Cloud in Sample Land Surveying

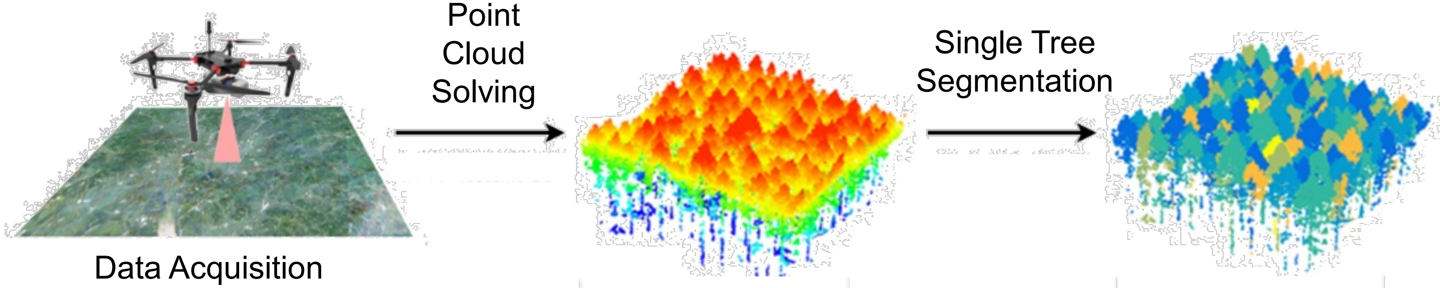

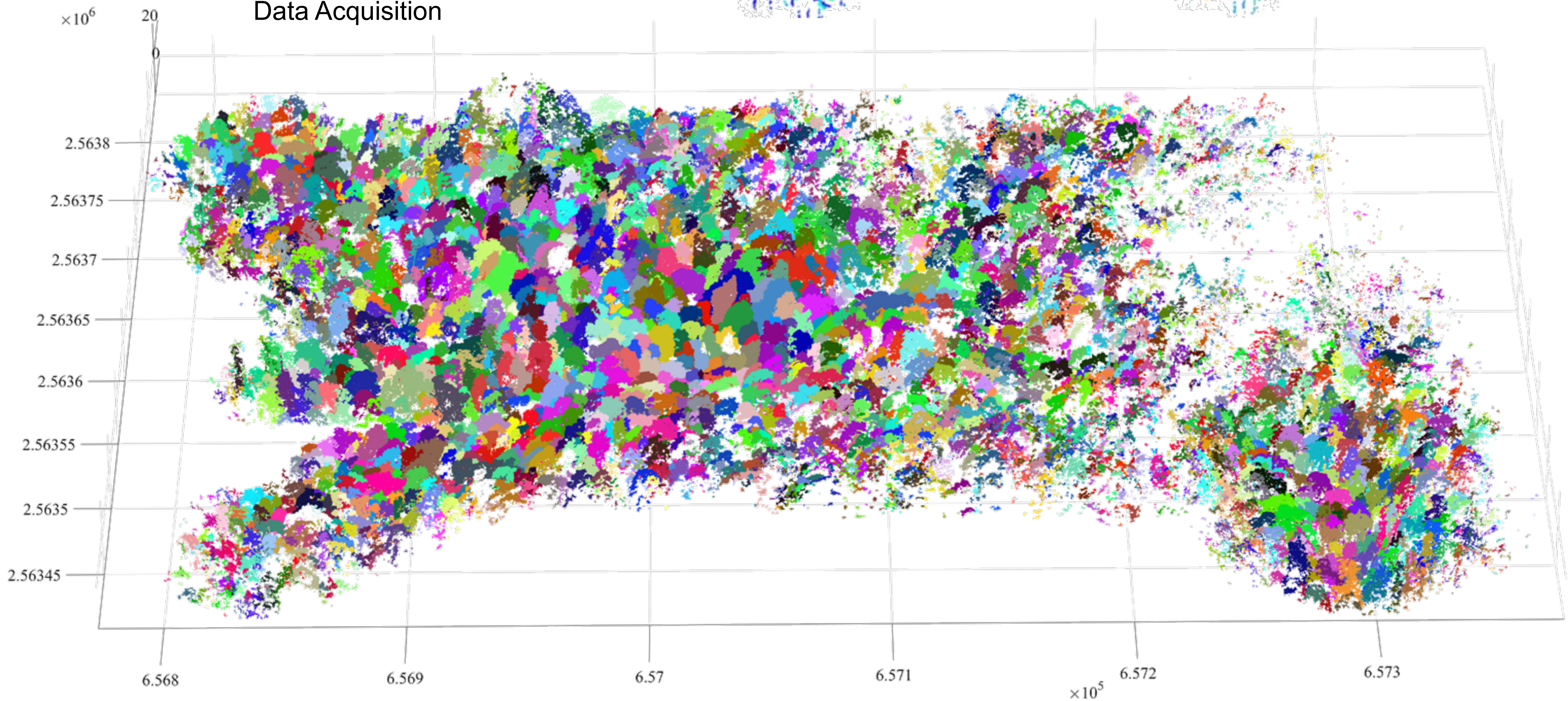

GT Wu et al. *Remote Sensing*. 2022

Characteristics of field canopy structure

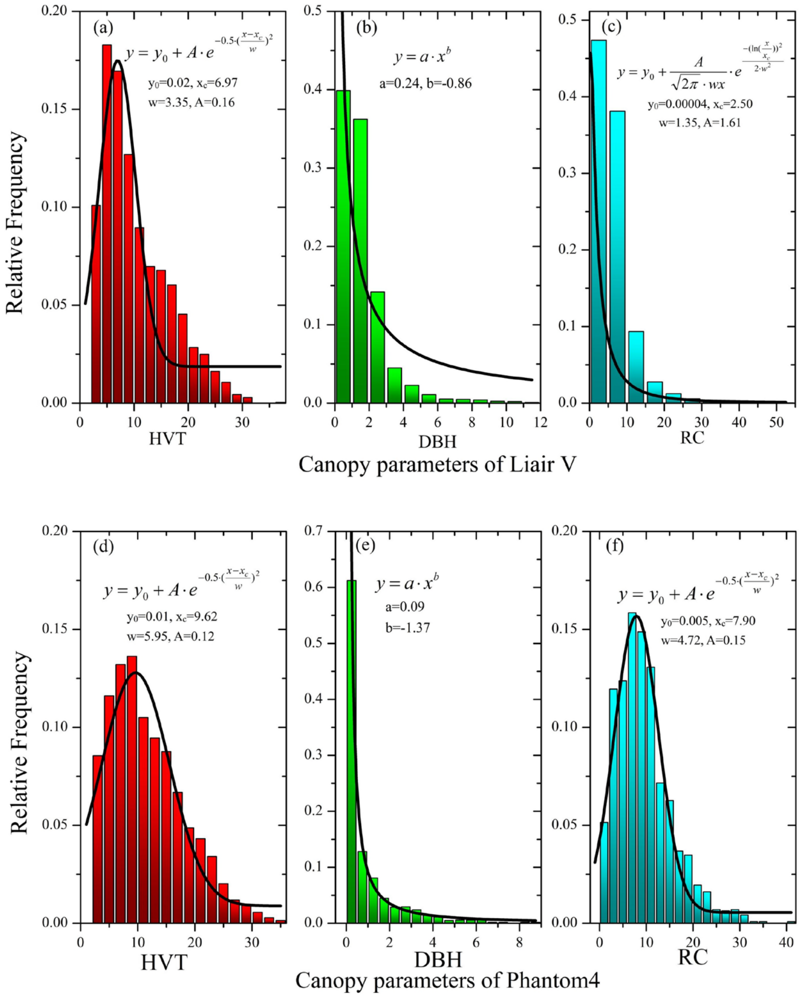

Average values of the canopy structure

	LPR	VPR	Observed (Reference)
Average tree height (HVT, m)	16.35 ± 2.19	16.02 ± 7.07	7.0~16.7
The diameter at breast height (DBH, cm)	2.22 ± 1.92	1.48 ± 1.60	5.1~21.9
Canopy radius (RC, m)	3.92 ± 1.78	4.80 ± 2.35	3.0~16.0
Leaf area index (LAI)	4.28 ± 2.38	0.48 ± 0.43	6.5 ± 0.7
Canopy cover	0.81 ± 0.18	0.48 ± 0.32	>0.8
Gap fraction	0.19 ± 0.18	0..52 ± 0.42	0.1~0.2

LPR: LiDAR Photogrammetry Results
VPR: Visible-light Photogrammetry Results

- Passive optical remote sensing has major limitations in establishing a link with vegetation.

Correction of canopy parameters by using fitting function

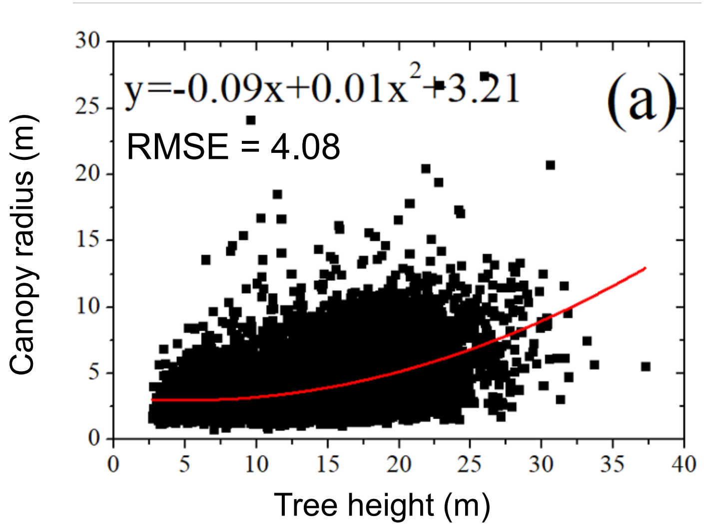

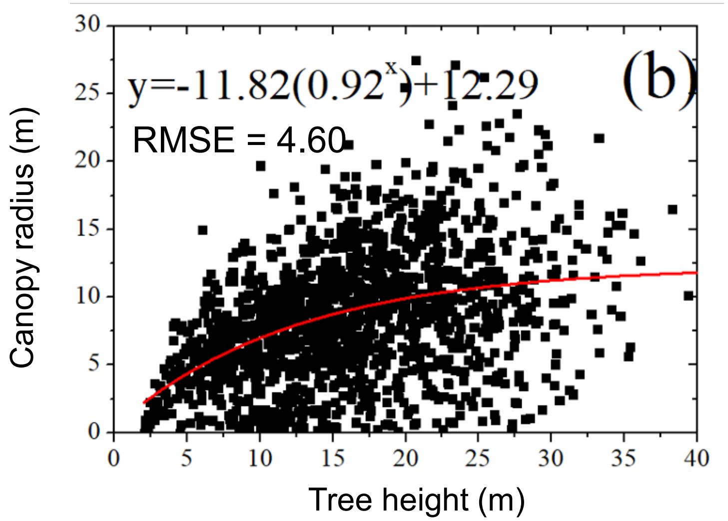

- Relationship between average tree height (HVT) and Canopy radius (RC) driven by (a) LPR and (b) VPR.
- Red lines indicate linear fits.

HVT and RC functions for Noah-MP inputs

Variables	Default	LPR	VPR
HVT	16.0	HVT from LPR	HVT from VPR
RC	1.4	$-0.09 \times HVT + 0.01 \times HVT^2 + 3.21$	$-11.82 \times 0.92^{HVT} + 12.29$

Results of the simulated canopy temperature and humidity profiles

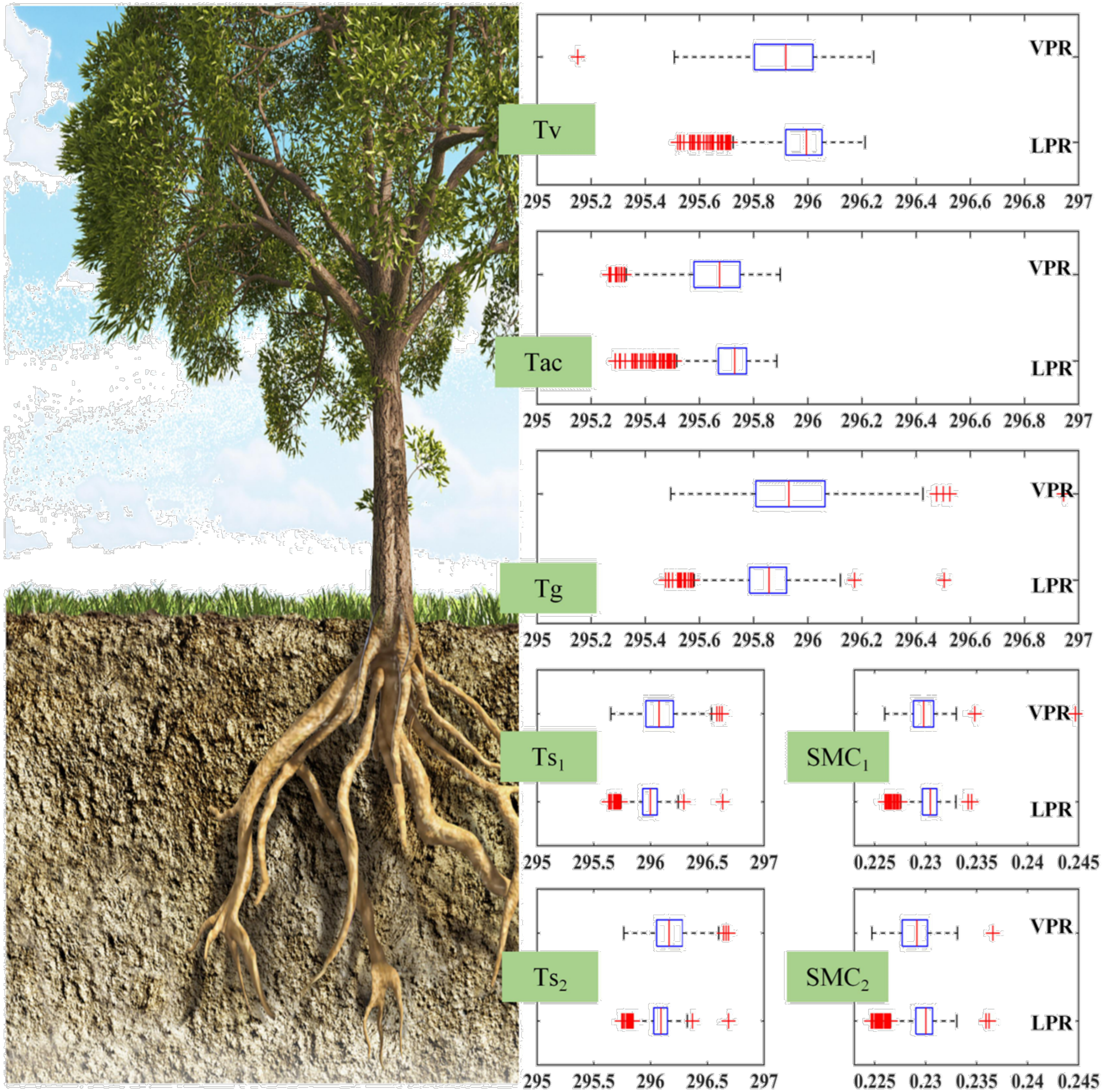

Diagnosis of the radiation and heat fluxes

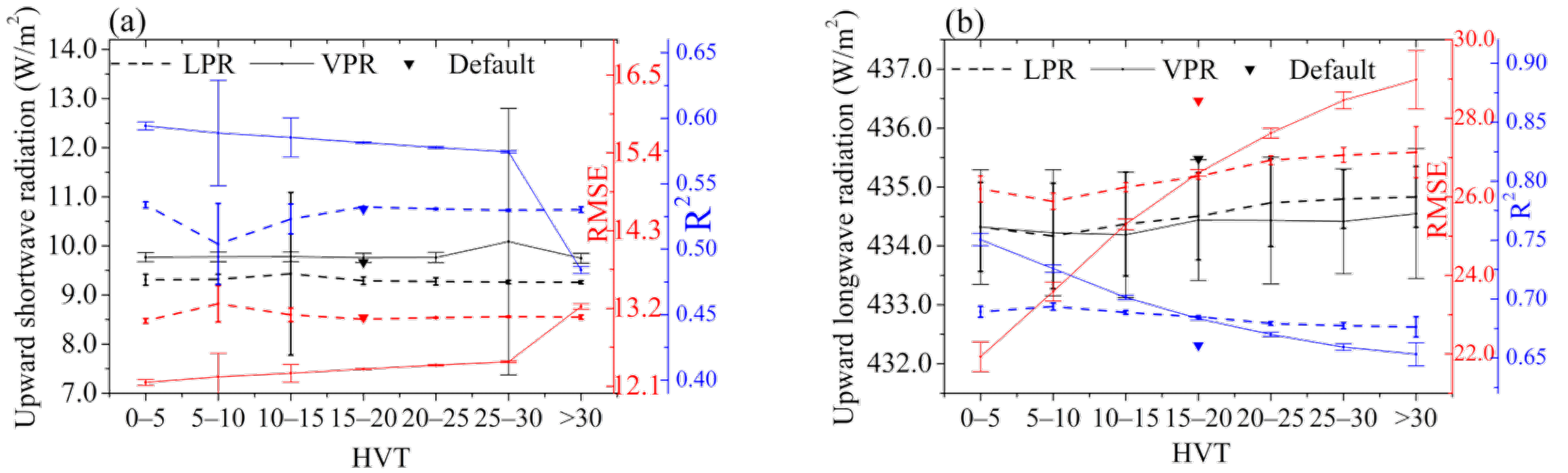

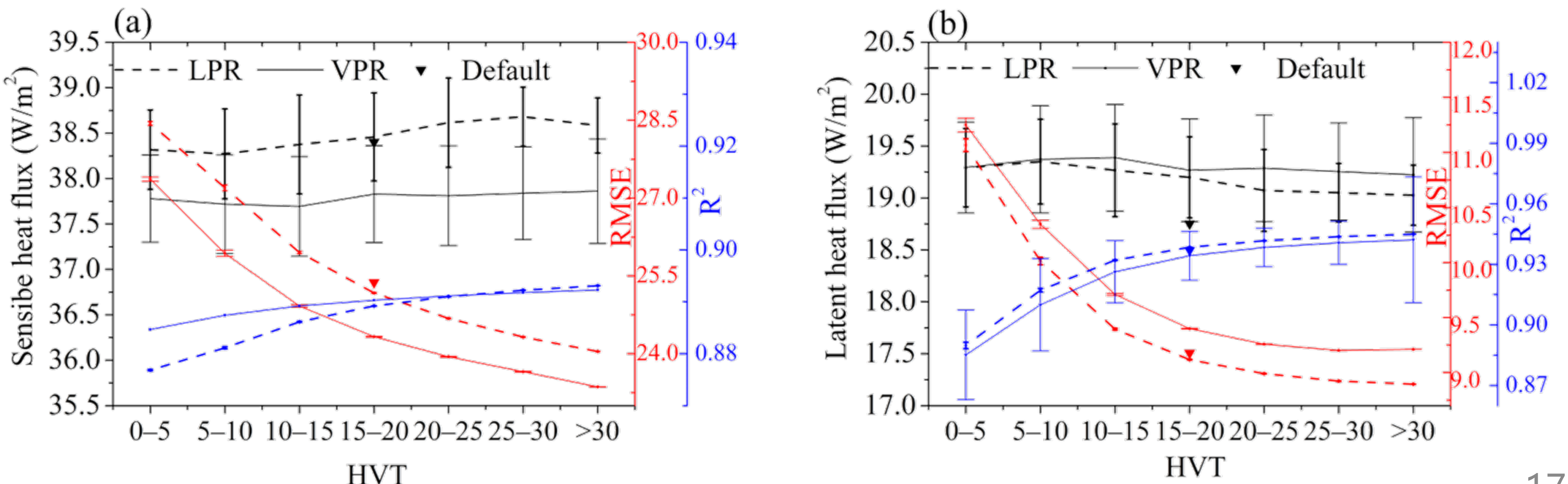

GT Wu et al. *Remote Sensing*. 2022

Parameters vs OPT_RAD option choice

Experimental name	Vegetation canopy parameters	Vegetation canopy structure programme options
D_1	Default	Three-dimensional (3D) canopy morphology
D_2		Non-vegetated gap
D_3		Coverage-based
LPR_1	LPR	Three-dimensional (3D) canopy morphology
LPR_2		Non-vegetated gap
LPR_3		Coverage-based
VPR_1	VPR	Three-dimensional (3D) canopy morphology
VPR_2		Non-vegetated gap
VPR_3		Coverage-based

Canopy 3D Morphology with LiDAR Photogrammetry Parameter inputs have Lower RMSE for radiation

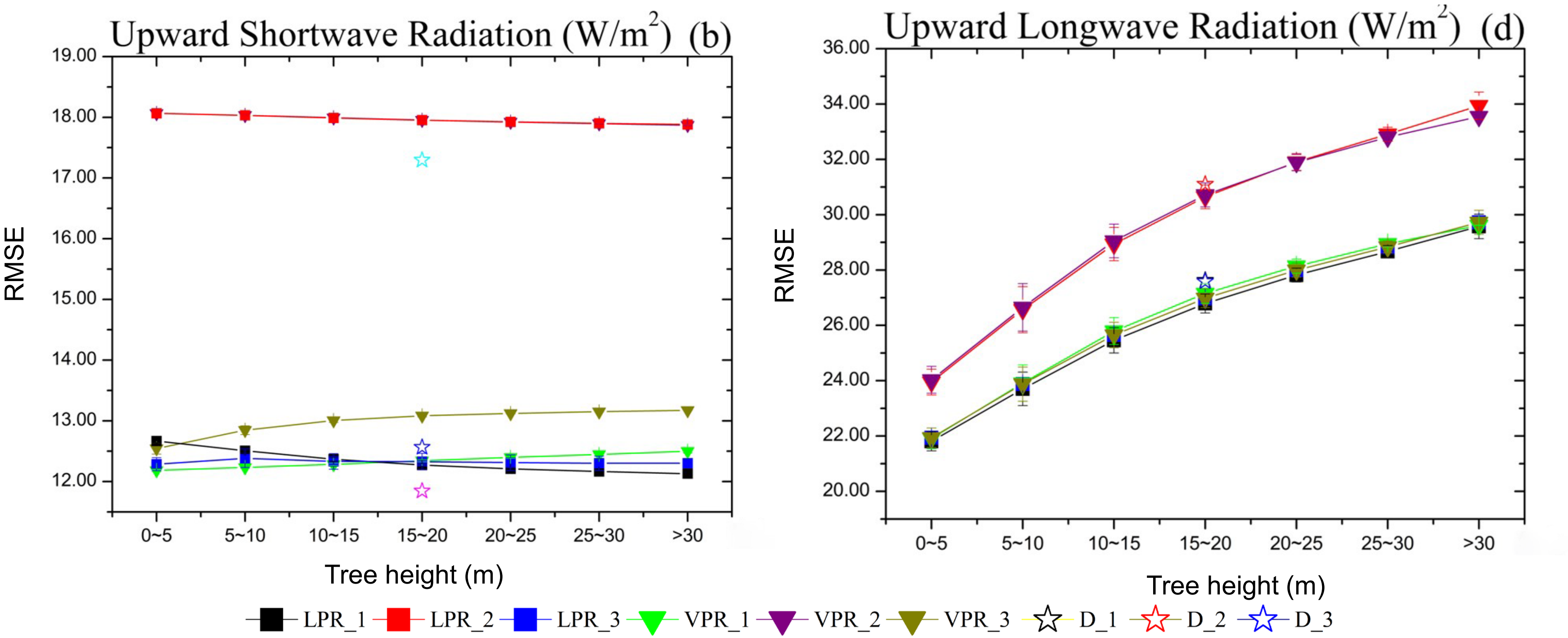

- The upward shortwave radiation and upward longwave radiation RMSEs simulated by the LPR are reduced by 9.5% and 3.6% compared to the VPR.

Canopy 3D Morphology with LiDAR Photogrammetry Parameter inputs have Lower RMSE for latent heat flux

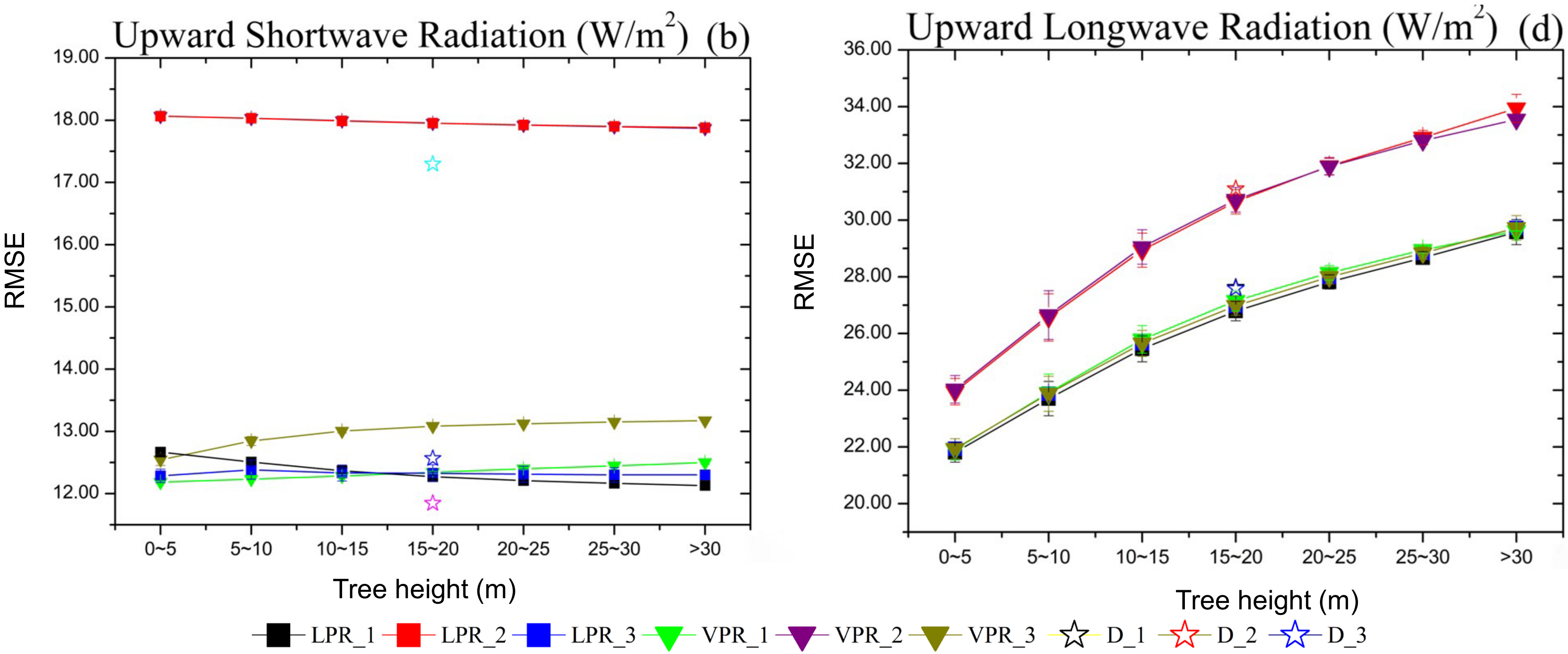

- The upward shortwave radiation and upward longwave radiation RMSEs simulated by the LPR are reduced by 9.5% and 3.6% compared to the VPR.

Current Mechanism

Considering canopy gaps

P_c: total canopy gap probability

$$P_c = min\begin{cases} 1 - F_{veg} \\ \boxed{P_{bc} + P_{wc}} \end{cases}$$

$$K_{open} = 0.05$$

K_{open}: gap fraction

F_{veg}: veg fraction

between-crown gap probability

$$P_{\mathrm{bc}} = e^{\frac{-\rho_{\mathrm{t}} \times \pi \times \boxed{r^2}}{\cos(\theta')^2}}$$

$$\rho_t = -\frac{\log(\max(1.0 - F_{veg}, 0.01))}{\pi \times r^2}$$

$$\theta' = \tan^{-1}[\frac{H_{top} - H_{bot}}{2r} \times \tan\theta]$$

r: tree crown radius
H_{top}: height to canopy top
H_{bot}: height to canopy bottom

within-Crown Gap Probability

$$P_{\mathrm{wc}} = (1 - P_{bc}) \times e^{\frac{-0.5 \times F_a \times (H_{\mathrm{top}} - H_{bot})}{\cos\theta}}$$

No canopy gaps

$$P_c = 0$$

$$K_{open} = 0$$

Further work 1: Expressing more refined canopy structure and processes in the model

Extractable from UAV-based photogrammetry:
Height, Length, Volume, Coverage
Canopy closure, Leaf area index, Gap rate, Biomass···

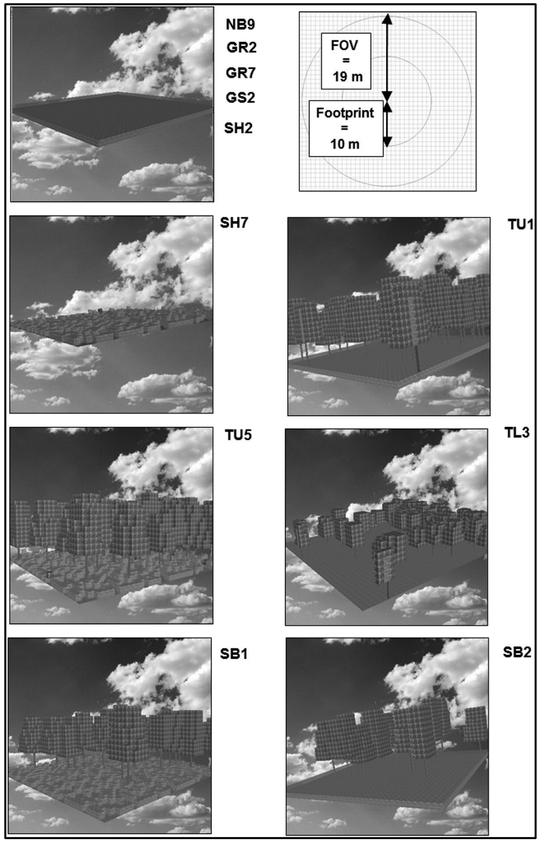

(Lamelas-Gracia et al., 2019)

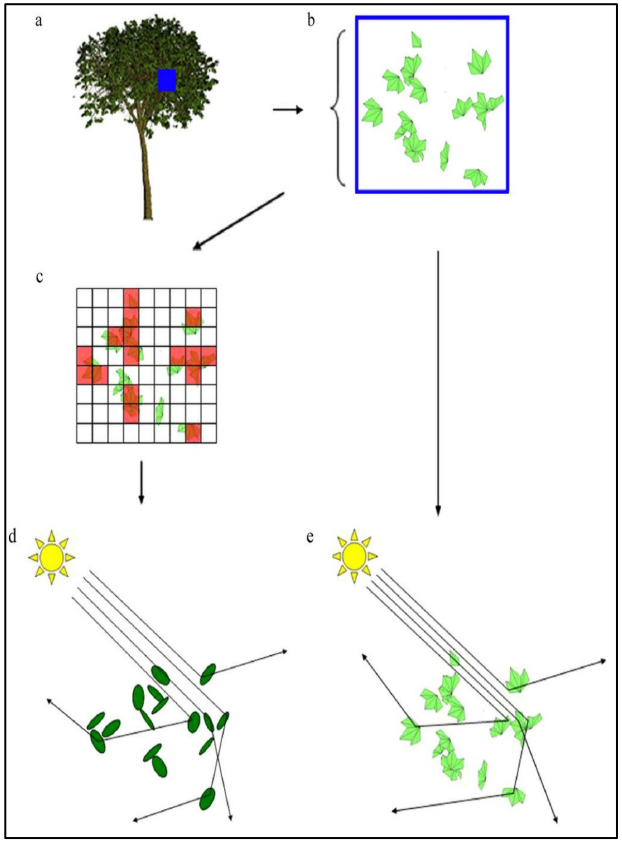

(Van der Zande et al., 2011)

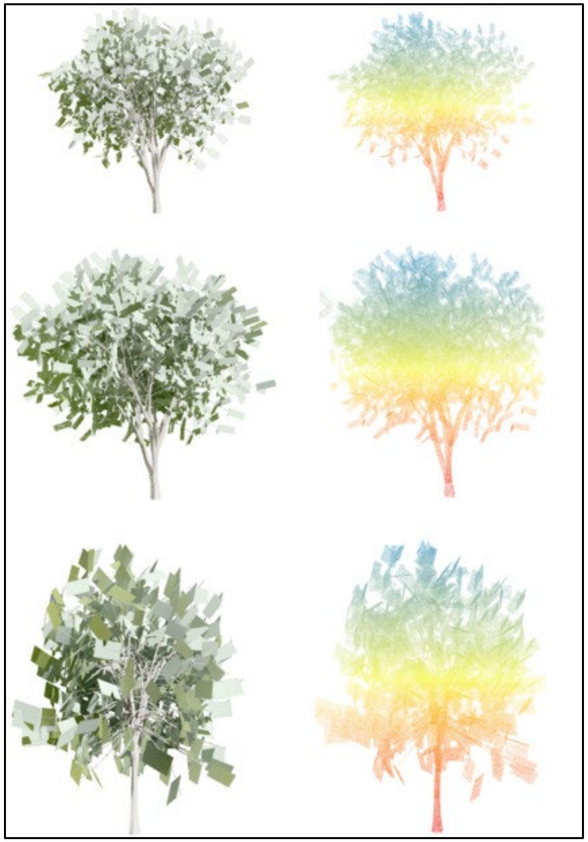

(Li et al., 2018)

Further work 2: expressing and comparing from other scales

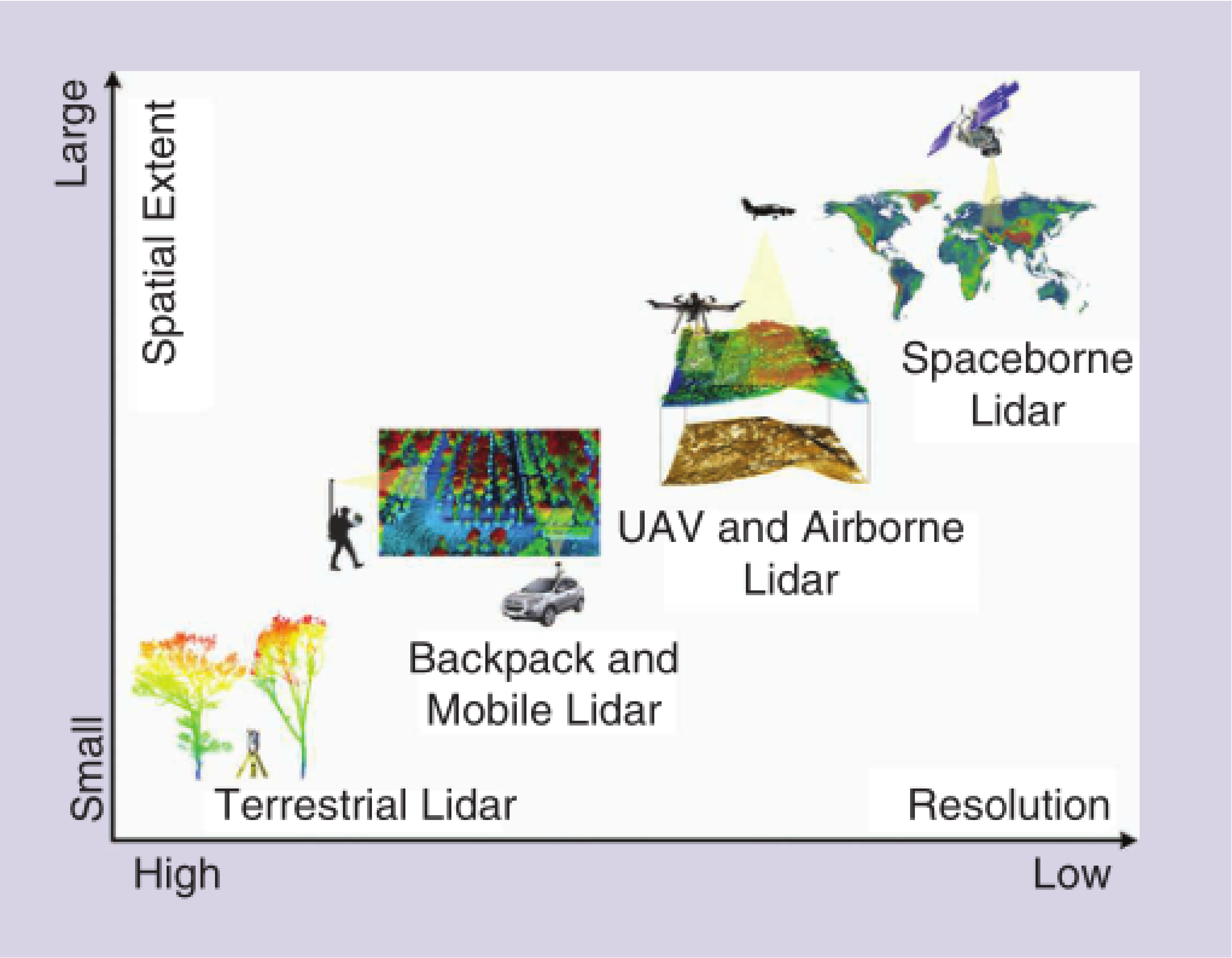

Related Papers

- M Chang, JC Cao, Qi Zhang, WH Chen, GT Wu, LP Wu, WW WANG, XM Wang*, Improvement of stomatal resistance and photosynthesis mechanism of Noah-MP-WDDM (v1.42) in the simulation of NO_2 dry deposition velocity in forests, **Geoscientific Model Development**, 2022. 15(2):787-801.
- GT W, YC Y, YB Y, JC Cao, YJ Bai, SJ Zhu, LP Wu, WW Wang, M Chang* and XM Wang, UAV-LiDAR Measurement of Vegetation Canopy Structure Parameters and Their Impact on Land–Air Exchange Simulation Based on Noah-MP Model, **Remote Sensing**, 2022. 14(13):2998.
- M Chang, SJ Zhu, JC Cao, BY Chen, Qi Zhang, WH Chen, SG Jia, Krishnan Padmaja, XM Wang*. Improvement and Impacts of Forest Canopy Parameters on Noah-MP Land Surface Model from UAV-Based Photogrammetry. **Remote Sensing**. 2020, 12, 4120.
- M Chang, WH Liao, XM Wang*, Q Zhang, WH Chen, ZY Wu. An optimal ensemble of the Noah-MP land surface model for simulating surface heat fluxes over a typical subtropical forest in South China. **Agricultural and Forest Meteorology**. 2019, 281: 107815.


THANKS!